ACS Macro Letters

Letter

Cite This: ACS Macro Lett. 2019, 8, 1528−1534

pubs.acs.org/macroletters

Molecular Architecture Directs Linear−Bottlebrush−Linear Triblock Copolymers to Self-Assemble to Soft Reprocessable Elastomers

Shifeng Nian,[†] Huada Lian,[‡] Zihao Gong,[†] Mikhail Zhernenkov,[§] Jian Qin,*[,‡] and Li-Heng Cai*[,†,∥,⊥]

[†]Department of Materials Science and Engineering, [∥]Department of Chemical Engineering, and [⊥]Department of Biomedical Engineering, University of Virginia, Charlottesville, Virginia 22904, United States

[‡]Department of Chemical Engineering, Stanford University, Stanford, California 94305, United States

[§]National Synchrotron Light Source-II, Brookhaven National Laboratory, Upton, New York 11973, United States

Supporting Information

ABSTRACT: Linear−bottlebrush−linear (LBBL) triblock copolymers represent an emerging system for creating multifunctional nanostructures. Their self-assembly depends on molecular architecture but remains poorly explored. We synthesize polystyrene-*block*-bottlebrush polydimethylsiloxane-*block*-polystyrene triblock copolymers with controlled molecular architecture and use them as a model system to study the self-assembly of LBBL polymers. Unlike classical stiff rod-flexible linear block copolymers that are prone to form highly ordered nanostructures such as lamellae, at small weight fractions of the linear blocks, LBBL polymers self-assemble to a disordered sphere phase, regardless of the bottlebrush stiffness. Microscopically, characteristic lengths increase with the bottlebrush stiffness by a power of 2/3, which is captured by a scaling analysis. Macroscopically, the formed nanostructures are ultrasoft, reprocessable elastomers with shear moduli of about 1 kPa, two orders of magnitude lower than that of conventional polydimethylsiloxane elastomers. Our results provide insights on exploiting the self-assembly of LBBL polymers to create soft functional nanostructures.

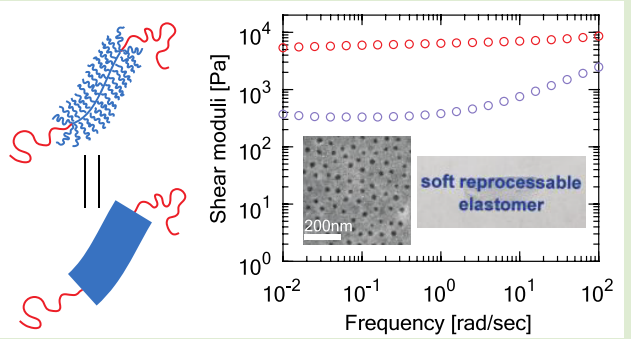

Block copolymers are made of two or more chemically distinct polymeric blocks linked by covalent bonds. A small incompatibility between the composing blocks is often sufficient to drive the copolymers to assemble to ordered nanostructures that find applications in many technologically important realms; examples include thermoplastic elastomers, templates for lithography, porous structures for filtration and separation, and drug carriers.[1−4] Key to functions and properties of the nanostructures is their characteristic length scales. The characteristic length scales afforded by classical flexible linear block copolymers is intrinsically small, however. It is largely determined by the molecular weight of polymers and is often below ∼100 nm.[5] Further increasing the molecular weight inevitably results in entanglement, which slows down the ordering kinetics.[8−10] Moreover, the entanglements act as effective cross-links and set an intrinsic lower limit in modulus, $\sim 10^6$ Pa, regardless of polymer species.[8] Achieving large domain sizes without forming entanglements would enable nanostructures with unprecedented properties and function. Examples include ultrasoft elastomers with stiffnesses mimicking that of biological tissues and photonic polymers for manipulating light.[5,6,7,11−15] Indeed, this is possible by using bottlebrush polymers whose entanglement molecular weight can be orders of magnitude larger than that of flexible linear polymers.[16,17] Moreover, synergizing the flexibility afforded by linear polymers, linear−bottlebrush−linear (LBBL) triblock copolymers have recently been found to self-assemble to a nanostructure that is mechanically soft while optically exhibiting structural color.[18] This highlights the potential of LBBL triblock copolymers as an emerging system for creating multifunctional nanostructures.

To fully unleash the potential of LBBL copolymers, the mechanisms of their self-assembly must be understood, and of importance is the role of the bottlebrush block. This is nontrivial, however, because of multiple physical parameters attributed to the molecular architecture of LBBL copolymers. In a LBBL polymer, the bottlebrush component is semiflexible, whereas the end blocks are flexible and incompatible with the bottlebrush block. The self-assembly of rigid, anisotropic molecules is driven by the minimization of excluded volume interactions, a phenomenon exemplified in liquid crystals and well-described by Onsager theory.[19,20] By contrast, the self-assembly of flexible block copolymers is driven by the

Received: September 13, 2019
Accepted: October 25, 2019
Published: November 1, 2019

DOI: 10.1021/acsmacrolett.9b00721
ACS Macro Lett. 2019, 8, 1528−1534

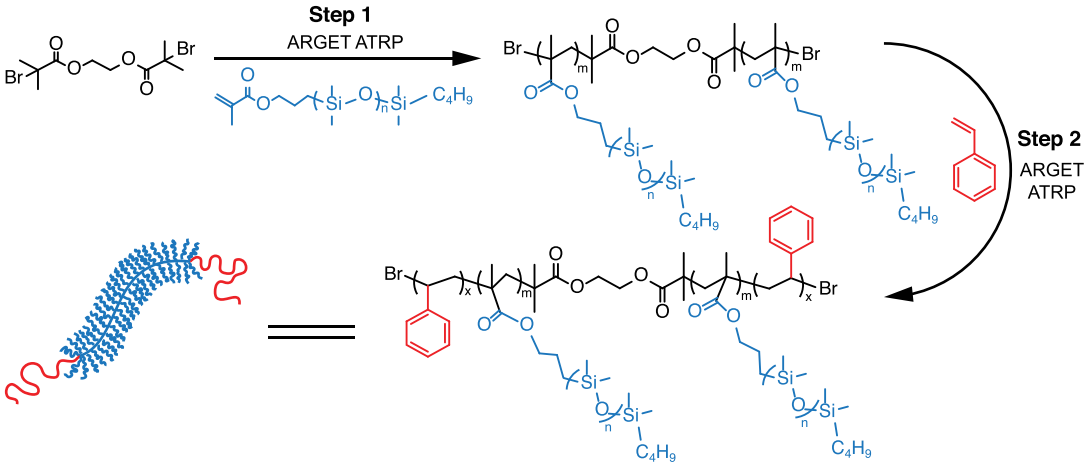

Figure 1. Synthesis of LBBL triblock copolymers. Step 1: ARGET ATRP of monofunctional PDMS macromonomers to form a bottlebrush PDMS. Step 2: ARGET ATRP of linear PS blocks.

minimization of interfacial free energy between the incompatible blocks while sacrificing conformational entropy of chains and is well-explained by self-consistent field theory.[8,21−26] Neither of these two mechanisms, however, is readily applicable to the self-assembly of LBBL triblock copolymers, in which both molecular stiffness and incompatibility are involved. As a result, it remains to be elucidated how the bottlebrush stiffness affects characteristic sizes of self-assembled nanostructures.

Here, we study the self-assembly of LBBL triblock copolymers by systematically tuning the stiffness of the bottlebrush block. We do so by developing a procedure that enables controlled synthesis of polystyrene-*block*-bottlebrush polydimethylsiloxane-*block*-polystyrene (PS-*b*-bbPDMS-*b*-PS) triblock copolymers. Using them as a model system, we fix both the weight fraction and the absolute molecular weight (MW) of the bbPDMS block, but increase the number of side chains per bottlebrush while decreasing their MW. This allows us to explore bottlebrush polymers spanning rigid, semiflexible, and flexible regimes. Characterizing the self-assembled nanostructures using transmission electron microscopy (TEM) and grazing-incidence small-angle X-ray scattering (GISAXS), we find that the characteristic length scales are determined by a single parameter—bottlebrush stiffness. The domain distance becomes nearly the same as the contour length of the bottlebrush when the middle bottlebrush block becomes semiflexible or stiff. However, unlike classic stiff rod-flexible linear block copolymers that are prone to form highly ordered nanostructures such as lamellae, for small PS weight fractions of ∼6%, LBBL polymers self-assemble to a sphere phase regardless of the bottlebrush stiffness. Moreover, consistent with scaling theory, the domain radius and distance increase with the bottlebrush contour length by a power of 2/3. Importantly, the molecular architecture enables LBBL polymers to self-assemble to ultrasoft, reprocessable elastomers with shear moduli on the order of 1 kPa, two orders of magnitude lower than that of conventional PDMS elastomers. These results provide insights on exploiting the self-assembly of LBBL polymers to create multifunction nanostructures.

The synthesis procedure we developed allows precise control over the molecular architecture of PS-*b*-bbPDMS-*b*-PS triblock copolymers (Figure 1; SI Materials and Methods). This procedure involves first the synthesis of the bbPDMS block, and then the two end linear PS blocks. For both steps, we exploit a recently developed activators-regenerated-by-electron-transfer (ARGET) atom transfer radical polymerization (ATRP), in which the catalysts are constantly regenerated from reducing organic reagents.[27,28] This improves the tolerance of oxygen and significantly reduces the required catalyst concentration, which are essential to the synthesis of bottlebrush PDMS with large molecular weight (MW). Moreover, unlike typical synthesis routes starting from monomers, we use an approach exploiting macromonomers to synthesize bottlebrush polymers. We use ARGET ATRP to polymerize monomethacryloxypropyl terminated polydimethylsiloxane (mMAPDMS) to create a PDMS bottlebrush (Step 1), which is used as a macro initiator to grow two end blocks of PS (Step 2). The completion of both steps results in a PS-*b*-bbPDMS-*b*-PS triblock copolymer.

Our approach for synthesizing PS-*b*-bbPDMS-*b*-PS triblock copolymers is versatile. It allows independent control over the MW of the PDMS side chain, the grafting density of the side chain by introducing spacer monomers, the number of side chains per bottlebrush, and the MW of the polystyrene blocks. During Step 1, by adjusting the molar ratio between the initiator and mMAPDMS macromonomers, we can control the number of side chains per bottlebrush. The size of mMAPDMS macromonomers can be controlled independently. During Step 2, tuning the amount of feed styrene monomers controls the MW of PS blocks. Therefore, the synthesis procedure allows exquisite control over the molecular architecture of the PS-*b*-bbPDMS-*b*-PS triblock copolymer.[29]

To investigate the roles of molecular stiffness on self-assembly, we fix the weight fraction of PS at about 6% and the MW of the bbPDMS at 500 kDa, but decrease the number of side chains per bottlebrush while increasing their MW. Samples with side chains of three MWs are created: 1 kDa (S^1_{500}), 5 kDa (S^5_{500}), and 10 kDa (S^{10}_{500}). Transmission electron microscopy (TEM; SI Materials and Methods, Tables S1 and S2) reveals that all samples self-assemble to a sphere phase in which the PS blocks form spherical domains (Figure 2a). Qualitatively, this is consistent with the self-assembly of linear PS-*b*-PDMS diblock copolymers, which microphase separate to a sphere phase with the weight fraction of A blocks below 14%.[30] Quantitatively, as the MW of side chains increases from 1 to 10 kDa, the radius of spherical PS domains, *r*, decreases

DOI: 10.1021/acsmacrolett.9b00721
ACS Macro Lett. 2019, 8, 1528−1534

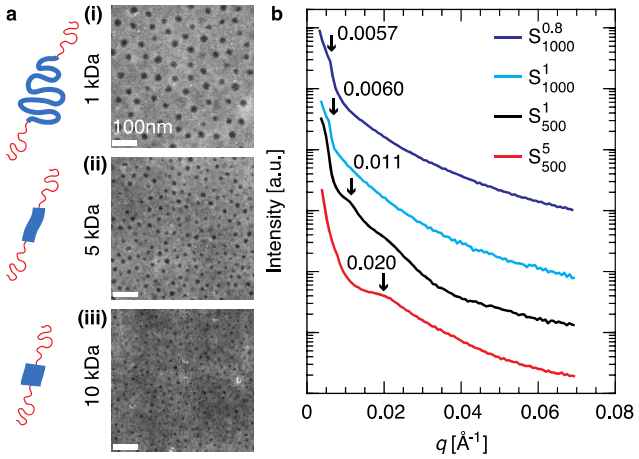

Figure 2. LBBL polymers self-assemble to form a sphere phase. (a) Representative TEM images of PS-*b*-bbPDMS-*b*-PS samples. The MW of bbPDMS is fixed at 500 kDa and the weight fraction of PS is about 6%, whereas the MW of side chains for bbPDMS increases from (i) 1 kDa, (ii) 5 kDa, to (iii) 10 kDa. The dark dots are PS domains, whereas regions of light color are bbPDMS. (b) GISAXS measurements reveal periodicity of LBBL samples. Details of samples are listed in Table 1.

from 11.9 ± 1.7 nm to 5.2 ± 1.0 nm, and the distance between the centers of neighboring PS domains, d, decreases from 53.6 ± 7.5 nm to 29.0 ± 10.2 nm. The estimated weight fraction of PS domains, $(2r)^3/d^3$, is consistent with that obtained from the weight fraction of PS blocks, which supports the assignment of the PS domains as spherical.

To further explore the ordering of nanostructures, we perform GISAXS measurements for LBBL samples (SI Materials and Methods, Table S3). The characteristic peaks shift to lower wavenumbers from q = 0.020 Å^{-1} to 0.011 Å^{-1} as the side chain MW decreases from 5 to 1 kDa (Figure 2b). Corresponding characteristic lengths are $2\pi/q$ = 28.5 and 57.1 nm, respectively, consistent with those measured by TEM. The variation in characteristic lengths for LBBL polymers with a fixed absolute and relative block MW is in stark contrast to the self-assembly of linear block copolymers, in which the characteristic lengths are constants.[1,21,22,31] Our results demonstrate that the molecular architecture of the bottlebrush determines the characteristic length scales of nanostructures self-assembled by LBBL copolymers.

The domain distance correlates to the contour length, L_{max}, of the bottlebrush, which is the maximum length to which the distance between neighboring PS domains can reach (SI Text). For sample S^1_{500}, the contour length is about 120 nm, four times of the bridging distance between two neighboring PS domains, $d - 2r \approx 30$ nm. The bridging distance approaches the contour length of the bottlebrush as the side chain MW increases. This phenomenon is reminiscent of the self-assembly of rod−coil block copolymers, in which the bridging distance between domains formed by the coil blocks is determined by the length of the stiff rod block.[32−34] Our results suggest that as MW of side chain increases, the self-assembly of LBBL polymers becomes more like that of rod−coil copolymers.

Indeed, a bottlebrush block with densely grafted side chains is analogous to a "fat" linear polymer.[35−38] The bottlebrush stiffness is quantified by the persistence length l_p, which is comparable to the size of the side chains R_{sc} (SI Text).[38,39] The ratio between the backbone contour length and the persistence length, $\kappa \equiv L_{max}/(2l_p)$, dictates the chain flexibility. The bottlebrush can be considered stiff for $\kappa < 1$, semiflexible for $\kappa \approx 1$, or flexible for $\kappa \gg 1$. In a melt, despite stretching attributed to steric repulsions, the conformation of a side chain is ideal, which increases with the side chain MW, M_{sc}, as $R_{sc} \sim (M_{sc})^{1/2}$ (SI Text). By contrast, the bottlebrush contour length is proportional to the number of side chains, $L_{max} \sim (M_{bb}/M_{sc})$, where M_{bb} is bottlebrush MW. Therefore, for bottlebrushes of a fixed MW, the ratio $\kappa \sim (M_{sc})^{-3/2}$ decreases rapidly with the increase of side chain MW.

We found that, for bottlebrush with MW of 500 kDa, the normalized bridging distance, $(d - 2r)/L_{max}$, increases with the decrease of κ (filled circles in Figure 3a). For relatively short

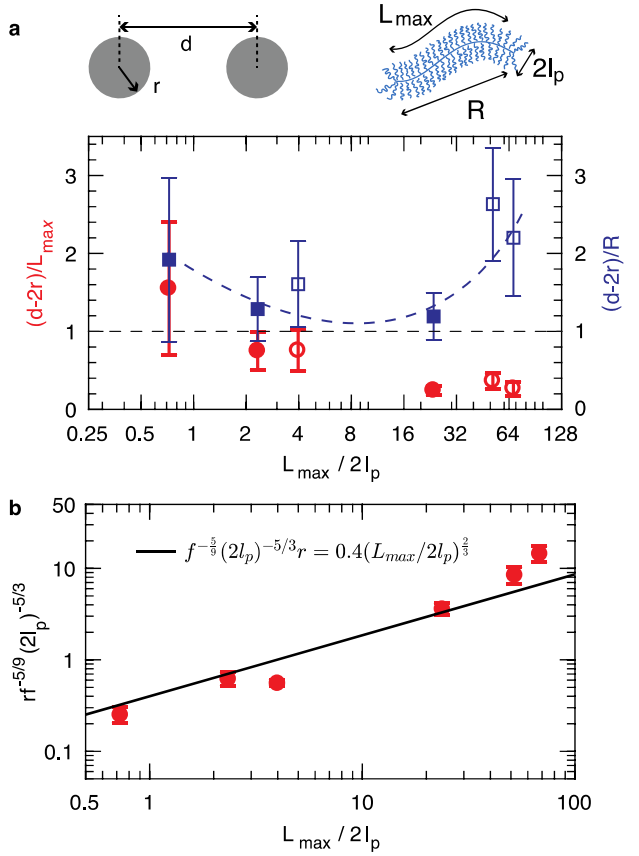

Figure 3. Increasing bottlebrush stiffness maximizes the domain distance in self-assembled nanostructures. (a) The ratio of the bridging distance to bottlebrush contour length, $(d - 2r)/L_{max}$, decreases with the increase of bottlebrush flexibility, $\kappa \equiv L_{max}/2l_p$, where l_p is the persistence length of the bottlebrush (red circles). By contrast, $(d - 2r)/R$, where R is the bottlebrush end-to-end distance calculated using molecular parameters of bottlebrush (SI Text) is always above 1 and becomes minimized at the value of $\kappa \approx 10$ (blue squares). The blue dashed line is for the guidance of eye. Filled symbols, LBBL polymers with MW of 500 kDa; empty symbols, MW of 1000 kDa. (b) The domain radius scales with the bottlebrush flexibility by a power of 2/3 (SI Text).

side chains of 1 kDa, the bottlebrush is flexible with $\kappa \approx 20$, and the bridging distance is about 1/4 of its contour length. The bottlebrush becomes fully stretched with $(d - 2r)/L_{max} \approx 0.8$ when it becomes semiflexible with $\kappa \approx 2$. This is different from the behavior of coil-semiflexible block copolymers, for which the interdomain distance is smaller than the contour

DOI: 10.1021/acsmacrolett.9b00721
ACS Macro Lett. 2019, 8, 1528−1534

Table 1. Parameters for LBBL Polymers and Their Self-Assembled Nanostructures[a]

	middle block			triblock			self-assembled nanostructure		
sample	M_{sc} (kDa)	n_{sc}	$Đ$	M_n (kDa)	f	$Đ$	d (nm)	r (nm)	G (Pa)
S^{1}_{500}	1	480	1.35	510	0.06	1.50	53.6 ± 7.5	11.9 ± 1.7	938
S^{5}_{500}	5	104	1.46	550	0.06	1.55	35.8 ± 6.4	7.8 ± 1.3	5367
S^{10}_{500}	10	47	1.44	490	0.04	1.51	29.0 ± 10.2	5.2 ± 0.9	907
$S^{0.8}_{1000}$	0.8	1212	1.37	990	0.02	1.42	125.5 ± 28.4	21.2 ± 4.2	374
S^{1}_{1000}	1	1050	1.43	1070	0.02	1.46	128.4 ± 27.0	15.2 ± 3.2	350
S^{5}_{1000}	5	180	1.70	922	0.02	1.75	42.3 ± 11.9	3.8 ± 0.3	1881

[a] M_{sc}, molecular weight of side chains; n_{sc}, number of side chains per bottlebrush; $Đ$, polydispersity index; f, weight fraction of end blocks; M_n, number average molecular weight; d, average distance between the centers of neighboring spherical domains; r, average radius of spherical domains; G, shear modulus of self-assembled nanostructures.

length of the semiflexible block.[40−43] Remarkably, when the bottlebrush becomes stiff, $\kappa \approx 0.7$, it is stretched to an extent larger than its contour length with $(d - 2r)/L_{max} \approx 1.6 \pm 0.8$. The average stretching ratio 1.6 could be an overestimate attributed to the widely distributed domain distance. Yet, within the measurement error this value agrees with the theoretical stretching limit 1.2 assuming fully stretched carbon−carbon bonds. The strongly stretched bottlebrush is likely because of the strong steric repulsion among long side chains, which generates a tension along the bottlebrush backbone to stretch chemical bonds; and in some cases, it is large enough to break a covalent bond.[44] Nevertheless, it is surprising that for a stiff middle block the LBBL polymers self-assemble to a sphere phase. This differs from the behavior of rod−coil copolymers, in which the rod-like blocks must be packed in space, and the way to do so without packing frustration[31] is to form highly ordered phases like lamellae.[33,45] We suspect this difference can be attributed to the flexibility of the side chains (Figure S16), which alleviates the packing frustration while the sphere phase is formed.[46] More quantitative understanding, however, is beyond the scope of this letter and will be the subject of further explorations. Nevertheless, our results demonstrate a clear threshold stiffness above which the bottlebrush is fully stretched in self-assembled nanostructures.

To further examine if the bottlebrush becomes less stretched when becoming more flexible, we synthesize three additional samples with MW of 1000 kDa: S^{5}_{1000} (200 sides chains of 5 kDa), S^{1}_{1000}, and $S^{0.8}_{1000}$. This allows us to create very flexible bottlebrush polymers with κ above 50. We find that $(d - 2r)/L_{max}$ becomes nearly a constant for $\kappa > 20$ (empty circles in Figure 3a). Remarkably, the ratio of the bridging distance to the calculated bottlebrush end-to-end distance R, $(d - 2r)/R$, exhibits a nonmonotonic dependence of the bottlebrush stiffness, as shown by the squares in Figure 3a (SI Text). As κ increases, the ratio first decreases and then increases, with a minimum at $\kappa \sim 10$. Moreover, the value of $(d - 2r)/R$ is always above 1. These suggest that, regardless of stiffness, the bottlebrush is always stretched, but the extent of stretching is minimized for an intermediate stiffness.

Although the extent of bottlebrush stretching exhibits a nonmonotonic dependence on the bottlebrush stiffness, both the domain distance and radius increase with the length of the bottlebrush (Figure 2a and Table 1). To rationalize this behavior, we develop a scaling theory for the observed spherical microstructures. We consider two types of free energy contributions: (1) the interfacial free energy between distinct domains and (2) the stretching free energy of the middle bottlebrush block. The stretching free energy of the end blocks is neglected because it is much smaller than that of the bottlebrush block (SI Text). The interfacial free energy is the product of the interfacial tension γ between PS and PDMS domains,[47] which correlates to the Flory−Huggins parameter χ,[8] and the interfacial area per unit volume f/r for spherical domains, in which $f \sim r^3/d^3$ is the weight fraction of PS blocks: $F_{int} \sim \gamma f/r$. The stretching free energy of the middle block is estimated by distinguishing two cases: (i) large κ, where the bottlebrush is Gaussian, coil-like, and (ii) small κ, where the bottlebrush is nearly fully extended, worm-like (SI Text). For a coil-like model, the density of the stretching free energy is given by $F_{ent} = \frac{k_BT}{V_c}\frac{d^2}{R^2} \approx \frac{k_BT}{V_C} f^{-2/3}\left(\frac{r}{R}\right)^2$, where V_c is the volume of a bottlebrush and $R^2 \approx l_p L_{max}$.

Minimizing the total free energy density, $F_{int} + F_{ent}$, gives $r \propto \left(\frac{\gamma}{k_BT}\right)^{1/3} f^{5/9} l_p L_{max}^{2/3}$. Consistent with this understanding, $rf^{-5/9}(2l_p)^{-5/3}$ scales with κ by a power of 2/3 (solid line in Figure 3b). This scaling relation is in essence the same as the 2/3 scaling with MW expected for the flexible linear polymers,[48] but takes into account the variation of architectural parameters unique to bottlebrush polymers using the number of effective Kuhn monomers per bottlebrush. Furthermore, assuming this scaling, in the stiff regime $R \approx L_{max}$ and, thus, $r/R \sim \kappa^{-1/3}$; in the flexible regime, $R \approx (l_p L_{max})^{1/2}$ and, thus, $r/R \sim \kappa^{-1/6}$, which rationalizes the nonmonotonic behavior seen in Figure 3a. Therefore, our experimental data conforms to the description of the coil-like rather than worm-like chain model. This challenges the classical understanding of treating densely grafted bottlebrush polymers as worm-like chains. Unlike typical worm-like chains such as double strand DNA for which the anisotropic ratio between the length and the cross-section of a Kuhn monomer is large of a value 50,[49] for a bottlebrush the anisotropic ratio is about 1; this implies that the effective Kuhn monomer of a bottlebrush is nearly spherical and thus the rationale of treating bottlebrush polymers as coil-like with $\kappa > 1$. Our results highlight the importance of controlling molecular architecture when exploiting the self-assembly of LBBL polymers to achieve large characteristic lengths, which are essential to the development of polymeric photonic crystals.[5,11−15]

The nanostructure self-assembled by LBBL polymers is similar to that of classical thermoplastic elastomers, in which the "hard" glassy domains form nodules that act as effective cross-links, whereas the "soft" elastic blocks act as network strands. Indeed, LBBL polymers self-assemble to a transparent solid (upper, Figure 4a). The solid nature is further confirmed by dynamic mechanical measurements (Figure 4b). Moreover, the equilibrium shear moduli for all samples are on the order of

DOI: 10.1021/acsmacrolett.9b00721
ACS Macro Lett. 2019, 8, 1528−1534

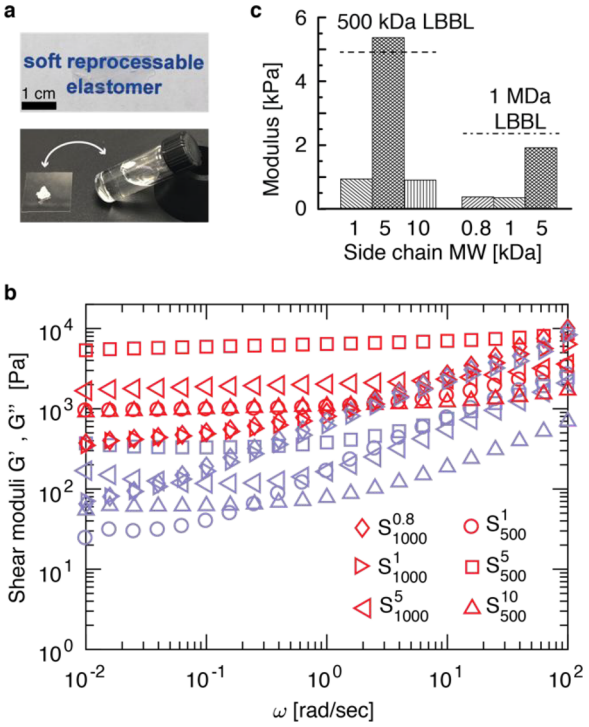

Figure 4. LBBL polymers self-assemble to optically transparent, mechanically soft, and reprocessable elastomers. (a) Upper, a representative optical image of the bulk material self-assembled by sample S^1_{500} at room temperature. Lower, the material is reprocessable using hexane as a solvent. The reprocessed material exhibits negligible changes in mechanical properties (Figure S14). (b) Storage (red symbols, G') and loss (blue symbols, G'') moduli of LBBL samples measured at 20 °C at a fixed strain of 0.5%. (c) Equilibrium shear moduli of LBBL samples at room temperature (bars) are on the order of 1 kDa and are much lower than the predicted values, k_BT per volume of a LBBL triblock copolymer, except for samples of 5 kDa side chains.

1 kPa, two orders of magnitude lower than 100 kPa for conventional PDMS elastomers, as shown in Figure 4c. This is because that the bottlebrush architecture prevents the formation of entanglements, enabling ultrasoft, solvent-free elastomers.[39] Furthermore, the shear modulus of sample S^5_{500} is consistent with the theoretical prediction for unentangled elastomers (dashed line in Figure 4c). The prediction is k_BT per volume of a block copolymer: $G_t = k_BTN_{Av}\rho/M \approx 4700$ Pa, in which k_B is Boltzmann constant, $T = 295K$ is absolute temperature, $\rho \approx 1$ g/cm^3 is the density, and $M = 5.5 \times 10^5$ g/mol is the molar mass of sample S^5_{500}. For the rest samples, however, the measured moduli are more than four times lower than the predictions (lines in Figure 4c). This is likely because of the formation of loops with two end linear blocks from the same triblock copolymers linking the same spherical nodule,[50−53] resulting in elastically ineffective network strands and thus reduced network stiffness.[54−56] And the probability of two ends to meet to form loops increases when the bottlebrush becomes either more flexible or shorter, as confirmed by larger deviations of measured stiffness from the prediction for more flexible samples (Figure 4c and Table 1). These results highlight the importance of controlling bottlebrush architecture to avoid network defects and thus enable prescribed mechanical properties. Nevertheless, consistent with previous findings, LBBL polymer self-assemble to supersoft, solvent-free elastomers with stiffness mimicking that of "watery" biological tissues.[57]

In summary, we have developed a method for controlled synthesis of linear-bottlebrush-linear triblock copolymers. At low weight fraction of end linear blocks, the triblock copolymers self-assemble to a sphere phase regardless of the bottlebrush stiffness. The bottlebrush is always somewhat prestrained, but there is an optimum stiffness at which the prestretching is minimized in the self-assembled nanostructures. Moreover, the variation of the characteristic lengths with the persistence length and the contour length of the middle block follows the prediction based on the coil-like stretching free energy. Furthermore, the bottlebrush architecture prevents the formation of entanglements, enabling soft elastomers with moduli on the order of 1 kPa, two orders magnitude lower than that of conventional elastomers formed by linear polymers. Yet, it is essential to control the bottlebrush stiffness to achieve more predictable mechanical properties. Many fundamental questions remain to be elucidated. For example, how does the competition between the bending energy of the middle bottlebrush block and the molecular incompatibility among the distinct blocks affect the self-assembly? Does the molecular prestraining of bottlebrush affect the macroscopic stiffness of the self-assembled elastomers? Because the cross-links are glassy domains that can either be dissolved in solvents or dissociate at high temperature, the elastomers are reprocessable (lower, Figure 4a and Figure S14) and thermoreversible. Can we exploit such a solvent/temperature triggered solid-to-liquid transition to apply the soft elastomers for additive manufacturing? These questions will be explored in future publications. Nevertheless, together with the versatility of the synthesis and the resulted soft, reprocessable elastomers, the understanding of molecular architecture directed self-assembly provides insights on exploiting bottlebrush-based copolymers to create multifunctional nanostructures.

EXPERIMENTAL SECTION

Polymer synthesis, sample preparation, and characterization are presented in the Supporting Information.

ASSOCIATED CONTENT

Supporting Information

The Supporting Information is available free of charge on the ACS Publications website at DOI: 10.1021/acsmacrolett.9b00721.

Materials, methods, additional characterization by ^{1}H NMR, GPC, GISAXS, and TEM, and supporting text including theoretical calculations and discussions (PDF)

AUTHOR INFORMATION

Corresponding Authors

*E-mail: liheng.cai@virginia.edu.
*E-mail: jianq@stanford.edu.

ORCID

Mikhail Zhernenkov: 0000-0003-3604-0672
Jian Qin: 0000-0001-6271-068X
Li-Heng Cai: 0000-0002-6806-0566

Notes

The authors declare no competing financial interest.

DOI: 10.1021/acsmacrolett.9b00721
ACS Macro Lett. 2019, 8, 1528−1534

■ ACKNOWLEDGMENTS

This work was supported by University of Virginia start-up fund and in part by Virginia Catalyst Foundation and UVA Center for Advanced Biomanufacturing. This research used the SMI beamline (12-ID) of the National Synchrotron Light Source II, a U.S. Department of Energy (DOE) Office of Science User Facility operated for the DOE Office of Science by Brookhaven National Laboratory under Contract No. DE-SC0012704. We thank Dr. Joshua Choi, Dr. Xiaodong Li, and Dr. Lin Pu for using lab equipment and Dr. Mingjiang Zhong for helpful discussions.

■ REFERENCES

(1) Bates, C. M.; Bates, F. S. 50th Anniversary Perspective: Block Polymers - Pure Potential. *Macromolecules* **2017**, *50* (1), 3−22.
(2) Hamley, I. W. In *Developments in Block Copolymer Science and Technology*; Hamley, I. W., Ed.; John Wiley & Sons, Ltd: Chichester, U.K., 2004.
(3) Hadjichristidis, N.; Pispas, S.; Floudas, G. *Block Copolymers: Synthetic Strategies, Physical Properties, and Applications*; Wiley-Interscience, 2003.
(4) Lodge, T. P. Block Copolymers: Past Successes and Future Challenges. *Macromol. Chem. Phys.* **2003**, *204* (2), 265−273.
(5) Edrington, B. A. C.; Urbas, A. M.; Derege, P.; Chen, C. X.; Swager, T. M.; Hadjichristidis, N.; Xenidou, M.; Fetters, L. J.; Joannopoulos, J. D.; Fink, Y.; Thomas, E. L. Polymer-Based Photonic Crystals. *Adv. Mater.* **2001**, *13* (6), 421−425.
(6) Runge, M. B.; Lipscomb, C. E.; Ditzler, L. R.; Mahanthappa, M. K.; Tivanski, A. V.; Bowden, N. B. Investigation of the Assembly of Comb Block Copolymers in the Solid State. *Macromolecules* **2008**, *41* (20), 7687−7694.
(7) Runge, M. B.; Bowden, N. B. Synthesis of High Molecular Weight Comb Block Copolymers and Their Assembly into Ordered Morphologies in the Solid State. *J. Am. Chem. Soc.* **2007**, *129* (34), 10551−10560.
(8) Rubinstein, M.; Colby, R. H. *Polymer Physics*; Oxford University Press: Oxford; New York, 2003.
(9) Graessley, W. W. *Polymeric Liquids and Networks: Structure and Properties*; Garland Science: New York, 2004.
(10) de Gennes, P.-G. *Scaling Concepts in Polymer Physics*; Cornell University Press, 1979.
(11) Urbas, A. M.; Maldovan, M.; DeRege, P.; Thomas, E. L. Bicontinuous Cubic Block Copolymer Photonic Crystals. *Adv. Mater.* **2002**, *14* (24), 1850−1853.
(12) Kang, Y.; Walish, J. J.; Gorishnyy, T.; Thomas, E. L. Broad-Wavelength-Range Chemically Tunable Block-Copolymer Photonic Gels. *Nat. Mater.* **2007**, *6* (12), 957−960.
(13) Park, C.; Yoon, J.; Thomas, E. L. Enabling Nanotechnology with Self Assembled Block Copolymer Patterns. *Polymer* **2003**, *44* (22), 6725−6760.
(14) Prasad, P. N. Polymers for Photonics. *J. Nonlinear Opt. Phys. Mater.* **1994**, *3* (4), 531−541.
(15) Rumi, M.; Bunning, T. J. Polymers in Photonics: Controlling Information by Manipulating Light. *J. Polym. Sci., Part B: Polym. Phys.* **2014**, *52* (3), 157.
(16) Sveinbjörnsson, B. R.; Weitekamp, R. A.; Miyake, G. M.; Xia, Y.; Atwater, H. A.; Grubbs, R. H. Rapid Self-Assembly of Brush Block Copolymers to Photonic Crystals. *Proc. Natl. Acad. Sci. U. S. A.* **2012**, *109* (36), 14332−14336.
(17) Liberman-Martin, A. L.; Chu, C. K.; Grubbs, R. H. Application of Bottlebrush Block Copolymers as Photonic Crystals. *Macromol. Rapid Commun.* **2017**, *38* (13), 1700058.
(18) Vatankhah-Varnosfaderani, M.; Keith, A. N.; Cong, Y.; Liang, H.; Rosenthal, M.; Sztucki, M.; Clair, C.; Magonov, S.; Ivanov, D. A.; Dobrynin, A. V.; Sheiko, S. S. Chameleon-like Elastomers with Molecularly Encoded Strain-Adaptive Stiffening and Coloration. *Science* **2018**, *359* (6383), 1509−1513.
(19) Vroege, G. J.; Lekkerkerker, H. N. W. Phase Transitions in Lyotropic Colloidal and Polymer Liquid Crystals. *Rep. Prog. Phys.* **1992**, *55* (8), 1241−1309.
(20) Onsager, L. The Effects of Shape on the Interaction of Colloidal Particles. *Ann. N. Y. Acad. Sci.* **1949**, *51* (4), 627−659.
(21) Bates, F. S.; Fredrickson, G. H. Block Copolymer Thermodynamics: Theory and Experiment. *Annu. Rev. Phys. Chem.* **1990**, *41* (1), 525−557.
(22) Fredrickson, G. H.; Bates, F. S. Dynamics of Block Copolymers: Theory and Experiment. *Annu. Rev. Mater. Sci.* **1996**, *26* (1), 501−550.
(23) Bates, F. S. Polymer-Polymer Phase Behavior. *Science* **1991**, *251* (4996), 898−905.
(24) Mai, Y.; Eisenberg, A. Self-Assembly of Block Copolymers. *Chem. Soc. Rev.* **2012**, *41* (18), 5969.
(25) Leibler, L. Theory of Microphase Separation in Block Copolymers. *Macromolecules* **1980**, *13* (6), 1602−1617.
(26) Fredrickson, G. H.; Helfand, E. Fluctuation Effects in the Theory of Microphase Separation in Block Copolymers. *J. Chem. Phys.* **1987**, *87* (1), 697−705.
(27) Fischer, H. The Persistent Radical Effect: A Principle for Selective Radical Reactions and Living Radical Polymerizations. *Chem. Rev.* **2001**, *101* (12), 3581−3610.
(28) Matyjaszewski, K.; Jakubowski, W.; Min, K.; Tang, W.; Huang, J.; Braunecker, W. A.; Tsarevsky, N. V. Diminishing Catalyst Concentration in Atom Transfer Radical Polymerization with Reducing Agents. *Proc. Natl. Acad. Sci. U. S. A.* **2006**, *103* (42), 15309−15314.
(29) Lee, H. il; Pietrasik, J.; Sheiko, S. S.; Matyjaszewski, K. Stimuli-Responsive Molecular Brushes. *Prog. Polym. Sci.* **2010**, *35* (1−2), 24−44.
(30) Chu, J. H.; Rangarajan, P.; Adams, J. L. M.; Register, R. A. Morphologies of Strongly Segregated Polystyrene-Poly(Dimethylsiloxane) Diblock Copolymers. *Polymer* **1995**, *36* (8), 1569−1575.
(31) Matsen, M. W.; Bates, F. S. Unifying Weak- and Strong-Segregation Block Copolymer Theories. *Macromolecules* **1996**, *29* (4), 1091−1098.
(32) Pryamitsyn, V.; Ganesan, V. Self-Assembly of Rod-Coil Block Copolymers. *J. Chem. Phys.* **2004**, *120*, 5824.
(33) Olsen, B. D.; Segalman, R. A. Self-Assembly of Rod−Coil Block Copolymers. *Mater. Sci. Eng., R* **2008**, *62* (2), 37−66.
(34) Olsen, B. D.; Segalman, R. A. Phase Transitions in Asymmetric Rod-Coil Block Copolymers. *Macromolecules* **2006**, *39* (20), 7078−7083.
(35) Liang, H.; Cao, Z.; Wang, Z.; Sheiko, S. S.; Dobrynin, A. V. Combs and Bottlebrushes in a Melt. *Macromolecules* **2017**, *50* (8), 3430−3437.
(36) Leuty, G. M.; Tsige, M.; Grest, G. S.; Rubinstein, M. Tension Amplification in Tethered Layers of Bottle-Brush Polymers. *Macromolecules* **2016**, *49* (5), 1950−1960.
(37) Dutta, S.; Pan, T.; Sing, C. E. Bridging Simulation Length Scales of Bottlebrush Polymers Using a Wormlike Cylinder Model. *Macromolecules* **2019**, *52* (13), 4858−4874.
(38) Paturej, J. J.; Sheiko, S. S.; Panyukov, S.; Rubinstein, M. Molecular Structure of Bottlebrush Polymers in Melts. *Sci. Adv.* **2016**, *2* (November), No. e1601478.
(39) Cai, L. H.; Kodger, T. E.; Guerra, R. E.; Pegoraro, A. F.; Rubinstein, M.; Weitz, D. A. Soft Poly(Dimethylsiloxane) Elastomers from Architecture-Driven Entanglement Free Design. *Adv. Mater.* **2015**, *27* (35), 5132−5140.
(40) Kumar, N. A.; Ganesan, V. Communication: Self-Assembly of Semiflexible-Flexible Block Copolymers. *J. Chem. Phys.* **2012**, *136* (10), 101101.
(41) Gao, J.; Tang, P.; Yang, Y. Non-Lamellae Structures of Coil-Semiflexible Diblock Copolymers. *Soft Matter* **2013**, *9* (1), 69−81.
(42) Koga, M.; Abe, K.; Sato, K.; Koki, J.; Kang, S.; Sakajiri, K.; Watanabe, J.; Tokita, M. Self-Assembly of Flexible-Semiflexible-

DOI: 10.1021/acsmacrolett.9b00721
ACS Macro Lett. 2019, 8, 1528−1534

Flexible Triblock Copolymers. *Macromolecules* **2014**, *47* (13), 4438−4444.
(43) Dalsin, S. J.; Rions-Maehren, T. G.; Beam, M. D.; Bates, F. S.; Hillmyer, M. A.; Matsen, M. W. Bottlebrush Block Coolymers: Quantitative Theory and Experiments. *ACS Nano* **2015**, *9* (12), 12233−12245.
(44) Panyukov, S.; Zhulina, E. B.; Sheiko, S. S.; Randall, G. C.; Brock, J.; Rubinstein, M. Tension Amplification in Molecular Brushes in Solutions and on Substrates. *J. Phys. Chem. B* **2009**, *113* (12), 3750−3768.
(45) Halperin, A. Rod-Coil Copolymers: Their Aggregation Behavior. *Macromolecules* **1990**, *23*, 2724−2731.
(46) Clair, C.; Lallam, A.; Rosenthal, M.; Sztucki, M.; Vatankhah-Varnosfaderani, M.; Keith, A. N.; Cong, Y.; Liang, H.; Dobrynin, A. V.; Sheiko, S. S.; Ivanov, D. A. Strained Bottlebrushes in Super-Soft Physical Networks. *ACS Macro Lett.* **2019**, *8* (5), 530−534.
(47) Biresaw, G.; Carriere, C. J.; Sammler, R. L. Effect of Temperature and Molecular Weight on the Interfacial Tension of PS/PDMS Blends. *Rheol. Acta* **2003**, *42* (1), 142−147.
(48) Hashimoto, T.; Fujimura, M.; Kawai, H. Domain-Boundary Structure of Styrene-Isoprene Block Copolymer Films Cast from Solution. 5. Molecular-Weight Dependence of Spherical Microdomains. *Macromolecules* **1980**, *13* (6), 1660−1669.
(49) Marko, J. F.; Siggia, E. D. Stretching DNA. *Macromolecules* **1995**, *28* (26), 8759−8770.
(50) Zhou, H.; Woo, J.; Cok, A. M.; Wang, M.; Olsen, B. D.; Johnson, J. A. Counting Primary Loops in Polymer Gels. *Proc. Natl. Acad. Sci. U. S. A.* **2012**, *109* (47), 19119−19124.
(51) Wang, R.; Alexander-Katz, A.; Johnson, J. A.; Olsen, B. D. Universal Cyclic Topology in Polymer Networks. *Phys. Rev. Lett.* **2016**, *116* (18), 188302.
(52) Zhong, M.; Wang, R.; Kawamoto, K.; Olsen, B. D.; Johnson, J. A. Quantifying the Impact of Molecular Defects on Polymer Network Elasticity. *Science* **2016**, *353* (6305), 1264−1268.
(53) Zhou, H.; Schön, E. M.; Wang, M.; Glassman, M. J.; Liu, J.; Zhong, M.; Díaz Díaz, D.; Olsen, B. D.; Johnson, J. A. Crossover Experiments Applied to Network Formation Reactions: Improved Strategies for Counting Elastically Inactive Molecular Defects in PEG Gels and Hyperbranched Polymers. *J. Am. Chem. Soc.* **2014**, *136* (26), 9464−9470.
(54) Takano, A.; Kamaya, I.; Takahashi, Y.; Matsushita, Y. Effect of Loop/Bridge Conformation Ratio on Elastic Properties of the Sphere-Forming ABA Triblock Copolymers: Preparation of Samples and Determination of Loop/Bridge Ratio. *Macromolecules* **2005**, *38* (23), 9718−9723.
(55) Karatasos, K.; Anastasiadis, S. H.; Pakula, T.; Watanabe, H. On the Loops-to-Bridges Ratio in Ordered Triblock Copolymers: An Investigation by Dielectric Relaxation Spectroscopy and Computer Simulations. *Macromolecules* **2000**, *33* (2), 523−541.
(56) Sunday, D. F.; Chang, A. B.; Liman, C. D.; Gann, E.; Delongchamp, D. M.; Thomsen, L.; Matsen, M. W.; Grubbs, R. H.; Soles, C. L. Self-Assembly of ABC Bottlebrush Triblock Terpolymers with Evidence for Looped Backbone Conformations. *Macromolecules* **2018**, *51* (18), 7178−7185.
(57) Levental, I.; Georges, P. C.; Janmey, P. A. Soft Biological Materials and Their Impact on Cell Function. *Soft Matter* **2007**, *3* (3), 299−306.

DOI: 10.1021/acsmacrolett.9b00721
ACS Macro Lett. 2019, 8, 1528−1534